DESIGNING ULTRASENSITIVE AND STRECHABLE STRAIN SENSORS BY TAILORED FRAGMENTATION OF CARBON-BASED CONDUCTORS

G. Lubineau, Y. Xin, X. Xu and J. Zhou

King Abdullah University of Science and Technology (KAUST), Physical Science and Engineering Division, COHMAS Laboratory, Thuwal 23955-6900, Saudi Arabia
Gilles.lubineau@kaust.edu.sa, cohmas.kaust.edu.sa

Keywords: Strain sensors, Carbon nanotubes, Sensitivity, Stretchability

ABSTRACT

There is an increasing demand for strain sensors with high sensitivity and high stretchability for new applications such as robotics or wearable electronics. However, for available technologies, the sensitivity of the sensors varies widely. These sensors are also highly nonlinear, making reliable measurement challenging. Here we introduce a new family of sensors composed of a cracked carbon nanotube structures embedded in an elastomer. Cracks are usually considered detrimental to the overall mechanical and electrical properties of materials. However, if these cracks can be controlled, they also have the potential for use in mechanical sensing applications. In this study, we demonstrate that strain sensors based on fragmented single-walled carbon nanotube (SWCNT) assemblies embedded in poly (dimethyl siloxane) (PDMS) can maintain their sensitivity at very high strain levels. Our strategy here is to develop a new family of sensors taking advantage of the special properties of fragmented carbon-nanoparticles based structures (papers and wires). We systematically describe how to control the fragmentation of the conductive CNT papers or wires for achieving high-performance strain sensors. This fragmentation based sensing system brings opportunities to engineer highly sensitive stretchable sensors.

1 INTRODUCTION

Stretchable conductive materials have continued to receive considerable attention with the rapid development of stretchable electronic devices as they have bring new solutions to achieve both conductivity and stretchability.[1-6] The important factors that govern the performance of the strain sensor is sensitivity, stretchability and linearity. In detail, the sensitivity is represented by the gauge factor (GF) and evaluated by the relative resistance change versus applied strain. High GF sensors are vital for small strain detection and open up opportunities for exploration of subtle strain detection. The stretchability is the maximum uniaxial tensile strain of the sensor before failure, which will determine the sensing strain range. The linearity is significant for stretchable strain sensors because nonlinearity makes the calibration process difficult. However, conventional strain sensors cannot achieve the combination of high sensitivity (GF>100), high stretchability (strain >100%) and linearity. This will limit the development of application in wearable electronics.

One of the most effective approaches for bringing stretchability to highly conductive and brittle materials is the formation of cracks in the material on stretchable substrates.[7-10] Here, we introduce a new strategy[11-13], using fragmented SWCNT papers or wires, to construct high-performance strain sensors. We first introduce cracks with controlled density to SWCNT assemblies by tuning the paper thickness, wire diameter, etc. The fragmented SWCNT assemblies embedded in PDMS substrate shows a maximum stretchability while maintaining a high sensitivity. Moreover, the dense and well-controlled network cracks enable a high linearity of the sensing response. The combination of high sensitivity, high stretchability and high linearity of the sensor will be vital for the development of stretchable electronics.

2 EXPERIMENTAL

2.1 Materials and samples. SWCNTs with 2.7 wt % COOH groups were purchased from CheapTubes, Inc. at over 90 wt % purity and containing more than 5 wt % multiwalled CNTs (MWCNT). SWCNT length ranged from 5 to 30 μm and their outer diameter ranged from 1 to 2 nm. The true density of these SWCNTs was 2.1 g/cm^3. Methanesulfonic acid (CH_3SO_3H) and SYLGARD 184 PDMS were purchased from Sigma Aldrich. 0.5 wt.% SWCNT dope was prepared by adding 0.2 g of SWCNTs into 40 g of CH_3SO_3H, sealed in a glass bottle, stirred for 5 min and bath sonicated using a Brason 8510 sonicator (250 W) (Thomas Scientific) for 60 min. The mixture was then stirred for 12 h at 500 rpm. SWCNT/CH_3SO_3H dispersions were vacuum filtrated through a ceramic filtration membrane (pore size: 20 nm, Whatman). Any remaining CH_3SO_3H was removed from the sample by washing it with water. The freestanding SWCNT paper was peeled away from the filter and cut into 30×3 mm^2 strips for producing the strain sensors. The first layer of 5.3 g PDMS (ratio of base to curing agent is 10:1) was poured onto a 10×10 cm^2 petri dish s and cured at 70 °C for 12 min to obtain a sticky substrate. The strips of SWCNT paper were transferred onto the 0.5-mm-thick sticky PDMS substrates; copper wires were connected to the SWCNT paper strips by silver epoxy. Next, the second layer of PDMS of equal weight was poured onto the sample and cured at 70 °C for 2 h to fully encapsulate the SWCNT paper.

2.2 Characterizations. Scanning electron microscopy (SEM) on SWCNT paper was performed using a Quanta 3D (FEI Company). The mechanical behavior of the SWCNT assemblies was measured by a 5944 Instron universal testing machine at a strain rate of 0.4 mm min^{-1} by a 5-N load cell. The reversible motion (stretching and relaxing) of the sample was controlled by a 5944 Instron machine. The whole sample region is glued except the 4-mm gap in the center. This 4-mm gap between the metal plates defines the effective length of the sample for determining the strain during the stretching. The change in electrical resistance of the specimen was monitored using a U1252B digital multimeter. Fragmentation was generated on each sample by loading it to 50% strain at a speed of 0.4 or 1.2 mm min^{-1}.

3 RESULTS AND DISCUSSION

3.1 Sensing strategy and structure

Figure 1a shows that the SWCNT assemblies are prepared by vacuum filtration to obtain SWCNT papers. To achieve the desired low-strength, low-stiffness SWCNT assemblies, a mild acid, CH_3SO_3H, was used to disperse SWCNTs so that the tube-to-tube interactions are insufficient to induce alignment. A porous structure of the SWCNT papers or wires with randomly distributed SWCNT networks can be observed in the SEM images shown in Figure 1b. This randomly oriented structure results in low-strength SWCNT assemblies that facilitate breakage of the fragile films. CNT papers are typically not stretchable (strain to failure is less than 5%); therefore, to introduce stretchability of the material, we embedded them into a PDMS substrate. By cutting the samples using a die, we were able to obtain standard dog-bone-shaped specimens (Figure. 1c).

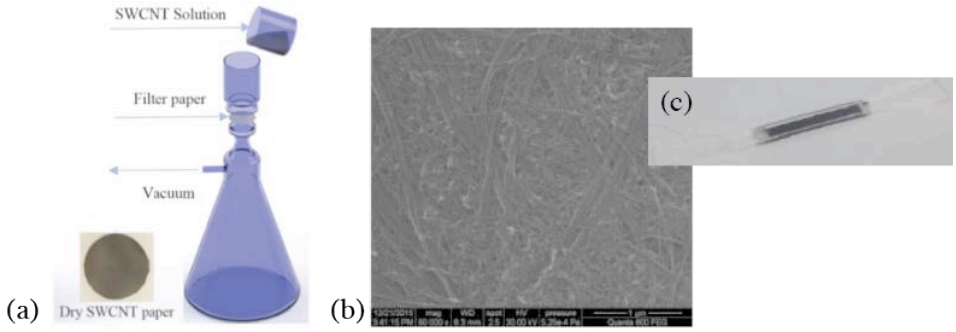

Figure 1: SWCNT paper or wire-based sensors. (a) Vacuum filtration of the SWCNT paper. (b) SEM images of the SWCNT paper and (c) PDMS encapsulated SWCNT paper strip.

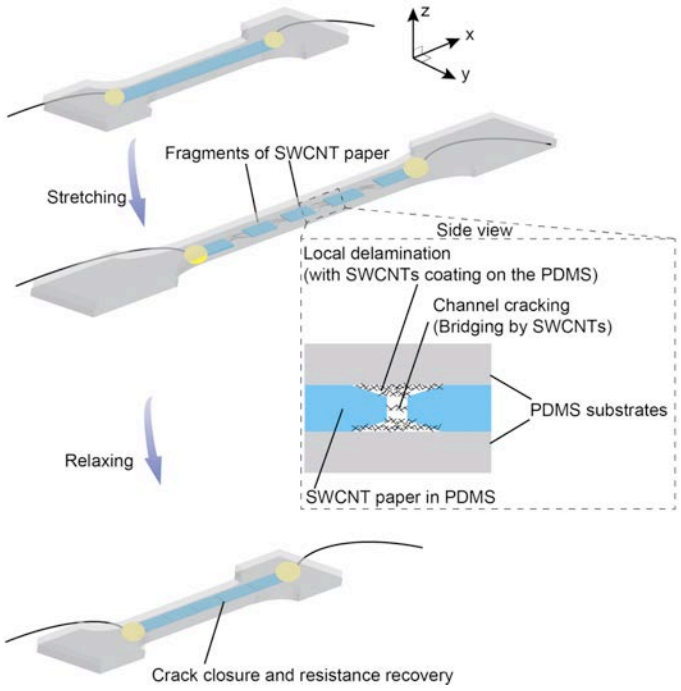

Figure 2: Strategy for fragmenting SWCNT assemblies in PDMS to produce high-sensitivity strain sensors. (a) A schematic presenting how SWCNT assemblies are fragmented in elastic substrates. (b) Illustrations of the mechanical sensing mechanism resulting from disconnection and connection of SWCNT networks in cracks.

Figure 2 demonstrates how a fragmented SWCNT-based sensor was stretched. When this sample is stretched, the SWCNT assemblies fragment, while the behavior of the surrounding PDMS remains reversible. When the strain is relaxed, cracks close but remains in the conductive medium. The disconnection and reconnection of SWCNT networks in cracks formed after stretching lead to sensing and resistance recovery, and become central to the sensing strategy.

3.2 Fragmented SWCNT paper for strain sensing

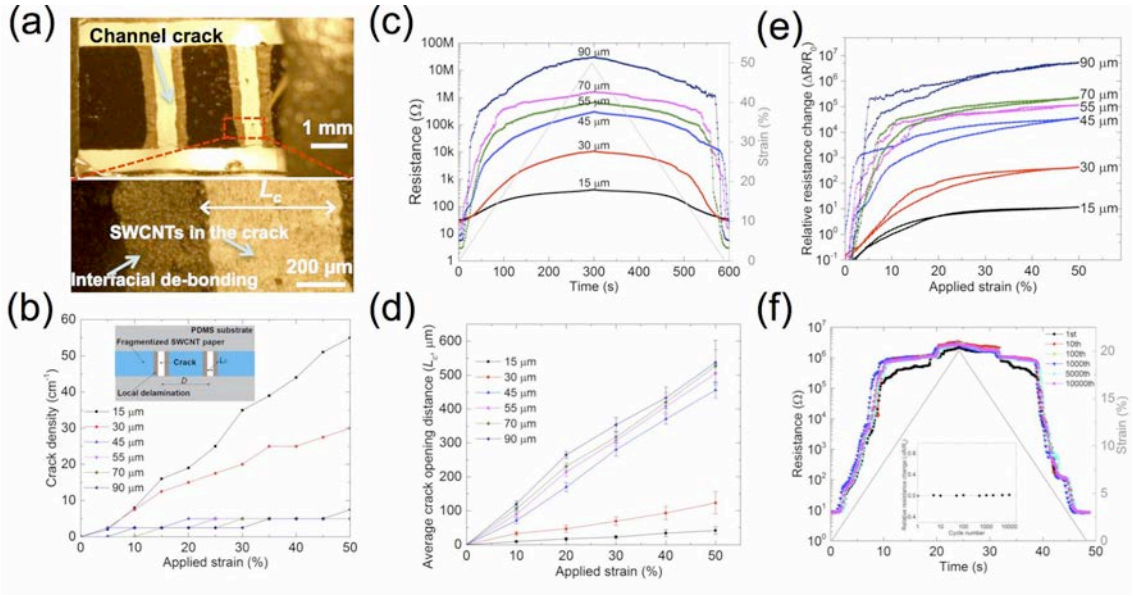

Figure 3:. Fragmented SWCNT paper in PDMS as a strain sensor. (a) Photograph of 45-µm-thick SWCNT paper embedded in elastic substrates after stretched to 50% strain. (b) Evolution of crack density with applied strain for samples of different thicknesses. We define in the inset image the average spacing (D) between the cracks. (c) Resistance changes by stretching and relaxing of strain sensors. (d) Increasing average crack opening distance (L_C) with increasing applied strain. (e) Relative resistance change versus applied strain of the SWCNT paper in elastic substrates during loading and unloading with a maximum applied strain of 50%. (f) Resistance changes versus strain for long-term cycle test: 1, 10, 100, 1000, 5000 and 10000 cycles at 0-20% strain at 2 mm min^{-1}. The Inset shows that the relative resistance change after relaxation from each cycle for a total of 10000 cycles, showing excellent long-term repeatability of the sensor.

The cracking mechanism is typical of degradation phenomenology in laminated structures. We used an SWCNT paper with a random, porous structure because its low strength and toughness make it easy to fragment. When the tensile load is increased, a pseudo-periodical pattern of channel cracks develops perpendicular to the principal loading direction (see Figure 3a). This is similar to the "transverse" cracking mechanism well know in laminated composites and to the channel cracking mechanisms in thin coatings, for which there are well-established micromechanical models.

The first stage of the degradation is a fragmentation process that is strongly dependent on thickness. Let us define the crack density (i.e., the number of cracks per unit length about the loading direction) as *1/D*, where *D* is the average spacing between the cracks, as shown in the inset image of Figure 3b. The evolution of crack density with strain is reported for the sample with different thicknesses. Two regimes can be observed: for "thin" papers (15 and 30 µm), channel cracks generally go only partially through the width and for "thick" papers (45, 55, 70 and 90 µm), very few cracks are observed, but those do run through the whole width of the sample. This is consistent with the classical micromechanics of channel cracking, where the usual distinction is done between an energy-guided regime for thin plies and a strength-guided regime for thick plies. The second stage of the degradation is the development of local delamination between the SWCNT paper and the PDMS substrate. Local delamination can be expected around crack tips because channel cracks cause severe out-of-plane stresses at the interfaces between the tips and the substrate. This process is dependent on the thickness of the ply: delamination is difficult to observe in the thin papers but obvious on the thick papers (45,

55, 70 and 90 μm). Furthermore, the degree of delamination depends on the balance between the energy release rate for channel cracking and the energy release rate for local delamination, the latter of which is more favorable in thick plies.

Figure 3c presents the strain-sensing behavior of strips of the fragmented paper in PDMS when the strain ranges from 0 to 50%. The resistance of the paper increases with applied strain for all samples. Moreover, the range of relative change in resistance ($\Delta R/R_0$) can be thickness controlled. This is very important for engineering the sensitivity of the strain sensor. At 50 % strain, the increase in resistance ranges from 100 Ω to 30 MΩ for 15-μm to 90-μm thick paper. The evolution of average crack opening distance, L_c, with strain is almost linear (Figure 3d), testifying to the linear elastic response of the sensor after fragmentation and relaxation. As expected, samples with larger opening distances exhibit larger resistance under strain (Figure 3c and d). For example, the resistance at a strain of 50 % of 15-μm and 45-μm samples are 400 Ω and 300 kΩ, respectively. The relatively small change in resistance of thin samples is attributed mainly to small fragments connecting the cracks, ensuring residual electronic transport. We then plot the relative change in resistance ($\Delta R/R_0$) with respect to the strain on Figure 3e. The sizeable change in resistance of 90-mm-thick SWCNT paper in PDMS enables us to obtain a GF of 2×10^6 at ε <5% and reach a record GF of 10^7 at ε = 50%. The high sensitivities across the low and high strain levels are important for wearable applications. The repeated opening and closing of the cracks led to reversible strain sensing with high sensitivity. Figure. 3f shows that the sensor displays a very high repeatability at 1, 10, 100, 1000, 5000, and 10000 cycles. After 10000 cycles at 20% strain, the resistance of the strain sensor (SWCNT paper thickness: 90 μm) remained nearly unchanged (inset in Figure 3f).

The stretchability could be dramatically improved by bringing high density of cracks containing conductive networks. Therefore, how to obtain the SWCNT paper with controlled crack density within an elastic substrate is a crucial point. Figure 4a show that partial cracks (partial meaning non extending through the whole thickness) on a SWCNT paper were obtained by a laser-engraving process. This approach is crucial to control the location of the cracks and to maintain the integrity and functionality of the SWCNT networks below the surface cracks. By decreasing the average spacing, D, between the cracks, the crack density, 1/D, can be increased. After embedding the laser-engraved SWCNT paper into a PDMS substrate, a roll-to-roll pressing process was repeatedly applied in clockwise and counterclockwise directions to fully initiate the fragmentation of SWCNT papers guided by surface cracks (Figure 4b). Upon roll-to-roll pressing, cracks were opened and propagated through thickness The average spacing, D, between the cracks was controlled at 2.0, 0.9, 0.6, 0.5 and 0.3 mm, correspond to different crack densities, 1/D, at 0.5, 1.1, 1.7, 2.0 and 3.3 mm^{-1}. These results prove that the laser engraving and roll-to-roll process is effective to control the cracking pattern. These through-thickness cracks will be a key element for the strain sensing. The crack-guided fragmentation in this study is superior to previous method by using only stretching of the SWCNT assembly, for which the crack spacing can only be coarsely controlled by engineering the thickness of the SWCNT paper (Figure 3). It is also advantageous over previously reported metal nanofilm fragmentation, in which cracks were formed with an uncontrollable manner through bending deformation. The ability to control the crack density in the SWCNT paper will be a prerequisite for tuning the stretchability of the sensor. For the sample of PDMS-embedded SWCNT paper with high crack density (3.3 mm^{-1}) (Figure 4c), when the sensor undergoes stretching, distributed cracks develops with crack size correlated to the applied strain. These cracks act as "switches" to adjust the density of the conductive networks of the sensor. As the strain ranges from 0 to 150%, the resistance of the paper increases with applied strain from 15 Ω to 1.2 MΩ.

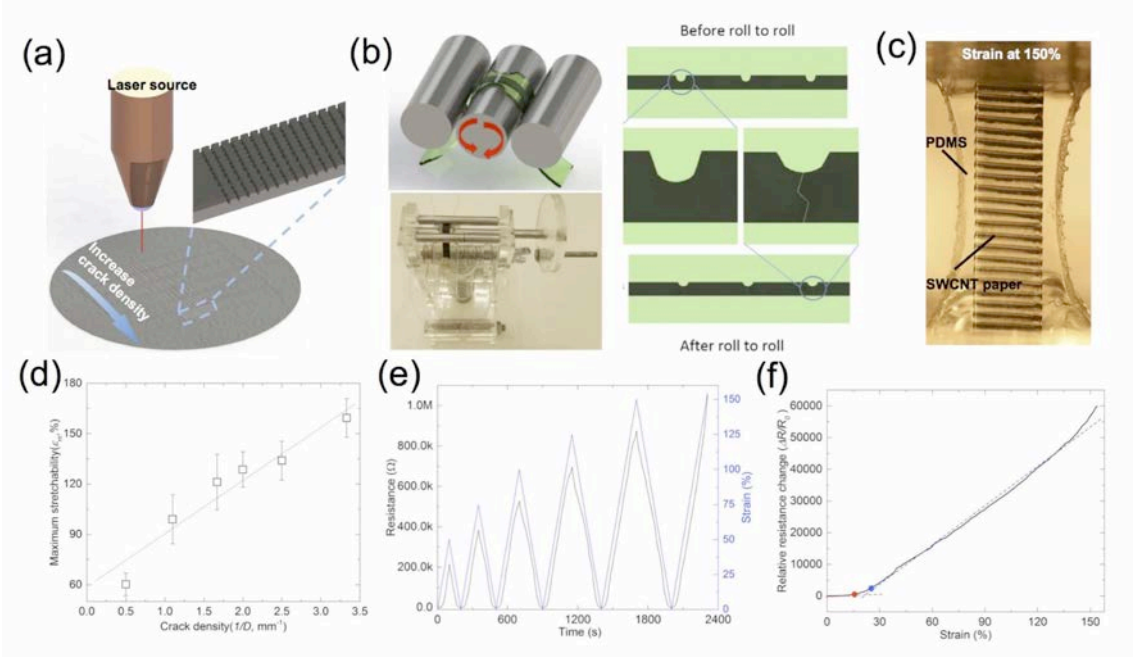

Figure 4:. Laser-engraved SWCNT paper for high-performance strain sensors. (a) Illustration image presents the laser-engraving process for generating partial cracks on the SWCNT paper. (b) An illustration and a real of roll-to-roll pressing device for the propagation of through-thickness cracks in SWCNT paper, respectively. Graphs on the right show the partial and through-thickness cracks before and after the roll-to-roll pressing, respectively. (c) Images of a typical, high crack density SWCNT paper in PDMS when stretched to 150% strain. (d) The increase of maximum stretchability of the sensors with crack density. (e) Resistance changes under incremental cyclic stretching/relaxing of a high crack density sensor (1/D = 3.3 mm^{-1}). The maximum stretchability of the sensor is determined to be 153%. (f) Relative change in resistance versus strain of the high crack density sensor (1/D = 3.3 mm^{-1}). Red and blue dashed lines are the fitting slopes for strain from 0 to 15% with a linearity of 0.98 and strain from 22 to 150% with a linearity of 0.96, respectively.

Figure 4d presents the maximum stretchability, ε_m, of the sensor with different crack density. The ε_m increased from 60% to 153% by increasing the crack density from 0.5 to 3.33 mm^{-1}, indicating the working range of the sensors at various crack densities. This trend suggests that the increase in crack density in SWCNT paper will dramatically increase the stretchability. In Figure 3, the stretchability of the SWCNT paper-based sensor is limited to 50-60% at a low crack density (1/D=0.5 mm^{-1}) due to the high-stress concentration around the cracks. The stress concentration near the cracks was high enough to result in an early failure of the PDMS substrate. Moreover, the sensor was showing an obvious nonlinearity due to the previously uncontrolled and quasi-random network of cracks. However, by introducing high crack density (1/D=3.33 mm^{-1}) to the SWCNT paper through laser-engraving and roll-to-roll pressing, the sensor show a maximum stretchability of 153% and a high linearity (Figure 4e). We then plot the relative change in resistance ($\Delta R/R_0$) on strain for the sample with the highest stretchability on Figure 4f. The change in resistance of this high crack density SWCNT paper in PDMS is $\Delta R/R_0 = 6.1 \times 10^4$ at 150%. The sensing behavior of the sample was characterized by two linear regions with 2 different slopes (strain from 0 to 15% with linearity of 0.98 and strain from 22 to 150% with linearity of 0.96), which reflects the GF at different strain range: the GF was 2.2×10^3 (0 to 15%) and 4.2×10^4 (22 to 150%). In comparison, conventional metal gauges have a GF around 2.0 at low strain ($\varepsilon < 5\%$).[1,2] The value is also higher compare with the performance of metal nanomaterials based stretchable sensors in both GF and maximum stretchability

4 CONCLUSION

We investigated here the advantages of using cracked structures in the design of ultrasensitive sensors. We started from a highly conductive film made of randomly oriented carbon nanotubes. Such a structure can be easily fragmented by a mechanical pretreatment such as pre stretching. It appeared that the performance of the sensor could be largely improved by carefully engineering the morphology and position of the cracks. This was achieved by introducing crack initiators by laser pre treatment.

Our future objective is to study the behavior is such sensors in the context of structural health monitoring in order to detect low amplitude vibrational changes.

REFERENCES

[1] Amjadi, M.; Kyung, K.; Park, I.; Sitti, M. Adv. Funct. Mater 2016, 26, 1678.

[2] Park, J.; You, I.; Shin, S.; Jeong, U. Chemphyschem 2015, 16, 1155–1163.

[3] Chortos, A.; Liu, J.; Bao, Z. A. Nat. Mater. 2016, 15, 937–950.

[4] Zhou, J.; Li, E. Q.; Li, R.; Xu, X.; Aguilar Ventura, I.; Moussawi, A.; Anjum, D.; Hed- hili, M. N.; Smilgies, D.; Lubineau, G.; Thoroddsen, S. T. J. Mater. Chem. C. 2015, 3, 2528– 2538.

[5] Zhou, J.; Mulle, M.; Zhang, Y. B.; Xu, X. Z.; Li, E. Q.; Han, F.; Thoroddsen, S. T.; Lu- bineau, G. J. Mater. Chem. C. 2016, 4, 1238–1249.

[6] Miura, H.; Fukuyama, Y.; Sunda, T.; Lin, B.; Zhou, J.; Takizawa, J.; Ohmori, A.; Kimura, M. Adv. Eng. Mater. 2014, 16, 550–555.

[7] Park, B.; Kim, J.; Kang, D.; Jeong, C.; Kim, K. S.; Kim, J. U.; Yoo, P. J.; Kim, T. Adv. Mater.2016, 28, 8130–8137.

[8] Kang, D.; Pikhitsa, P. V.; Choi, Y. W.; Lee, C.; Shin, S. S.; Piao, L. F.; Park, B.; Suh, K. Y.;Kim, T. I.; Choi, M. Nature 2014, 516, 222–226.

[9] Yang, T.; Li, X.; Lin, S.; Lao, J.; Shi, J.; Zhen, Z.; Li, Z.; Zhu, H. Mater. Horiz. 2016, 3,248–255.

[10] Liu,Z.Y.;Qi,D.P.;Guo,P.Z.;Liu,Y.;Zhu,B.W.;Yang,H.;Liu,Y.Q.;Li,B.;Zhang,C.G.;Yu, J. C.; Liedberg, B.; Chen, X. D. Adv. Mater. 2015, 27, 6230–6237.

[11] Xin, Y.; Zhou, X.; Xu, X.; Lubineau, G. Submitted. (2017).

[12] Zhou, J.; Yu, H.; Xu, X.; Han, F,; Lubineau, G. *ACS Appl. Mater. Interfaces*, 2017, 9(5), 4835-4842.

[13] Zhou, J.; Xu, X.; Yu, H.; Lubineau, G.. *Nanoscale*, 2017, **9**, 604-612.